COO-4246-5

MICROSTRUCTURAL EFFECTS IN ABRASIVE WEAR

Quarterly Progress Report
for the period 15 March 1978 - 15 June 1978

Nicholas F. Fiore, Joseph P. Coyle and Stephen Udvardy

Department of Metallurgical Engineering and Materials Science
Notre Dame, IN 46556

NOTICE
This report was prepared as an account of work sponsored by the United States Government. Neither the United States nor the United States Department of Energy, nor any of their employees, nor any of their contractors, subcontractors, or their employees, makes any warranty, express or implied, or assumes any legal liability or responsibility for the accuracy, completeness or usefulness of any information, apparatus, product or process disclosed, or represents that its use would not infringe privately owned rights.

1 July 1978

Prepared for

U. S. Department of Energy

Under Contract No. EF-77-S-02-4246

DISTRIBUTION OF THIS DOCUMENT IS UNLIMITED

DISCLAIMER

CONTENTS

ABSTRACT

The objective of this research is to correlate abrasive wear with microstructure in a series of alloy white irons and a series of Co-base powder metallurgy (PM) alloys. Effort this quarter has centered on the PM alloys. Low-stress abrasion resistance has been found to increase in a general way with hardness, whereas gouging wear resistance has been found to correlate to a significantly lesser extent. For gouging wear in particular, increasing hardness, carbon and alloy content are inefficient means to increase wear resistance.

The low-stress wear scar microtopography has been measured for each of the six alloys studied. In general, alloys with high wear resistance have smoother wear scars.

The microstructures of the alloys, which consist of an array of M_7C_3 (and in some cases $M_7C_3 + M_6C$) carbides in a FCC Co-base matrix, have been characterized by conventional optical and quantitative metallographic techniques. Both low stress and gouging wear resistance pass through a maximum at intermediate carbide volume fractions. This gives quantitative evidence of the inefficiency of excessive alloying to generate wear resistance. It suggests that for these alloys low-stress and gouging abrasion may be covered by common flow-fracture phenomena.

1. OBJECTIVE AND SCOPE

The objective of this research is to establish quantitative relations between microstructure and wear resistance of low-to-high Cr white irons and Co-base powder metallurgy (PM) alloys commonly used in coal conversion processes. The program involves study of gouging wear resistance, such as is necessary in mining operations, and low-stress abrasion resistance, such as required in coal and coal-product handling and transfer operations. The objective has both applied and basic aspects. On the practical side, the establishment of the optimum microstructures for wear resistance will allow (and is already beginning to allow) design engineers to make more effective decisions regarding candidate alloys for coal-related processes. From the basic viewpoint, the establishment of a better understanding of the physical and mechanical metallurgy of wear may lead in the longer run to the development of more economical and effective wear-resistant alloys.

The project has been in existence for about 15 months, during which time most of the testing and analysis has been conducted on the white irons. The majority of this, the fifth project quarterly report, is devoted to test results on the Co-base PM alloys.

2. TASKS AND PROGRESS

2.1. Task I - Preparation of Test Matrix

Task completed 6 June 1977.

2.2 Task II - Preparation of Materials

Task completed 15 March 1978.

The white iron and Co-base alloy materials have been obtained. The compositions, heat treatments and microstructures of the white irons have been discussed in the last quarterly report, COO-4246-4. A similar discussion for the

Co-base alloys will be given in this report.

2.3 Task III - Wear Testing

2.3.1 Composition and Structure of Co-base PM Alloys

As stated earlier, emphasis in this report will be placed on the abrasion resistance of the Co-base alloys. The six alloys chosen, whose chemical compositions are listed in Table I, are among the most erosion and erosion-corrosion resistant materials commercially available. In addition to being commercially relevant, the series of alloys comprise an interesting system for study since they span a range of increasing carbide volume fraction in matrices of increasing solid solution strengthener content (Table II).

The alloys have been subjected to low-stress rubber-wheel abrasion testing (RWAT) and gouging abrasion testing (GAWT) in an effort to correlate wear resistance with other mechanical properties and with metallurgical structure and composition.

2.3.2 Rubber-Wheel Abrasion Testing

As is indicated in Table II the Co-base PM alloys represent a series of increasing carbide and/or increasing matrix solid-solution strengthener content. RWAT tests with SiO_2 abrasive have been completed on the series, and the test results are displayed in Figures 1 and 2. In Figure 1 the weight loss data are displayed in histogram form, with increasing carbide and/or matrix alloy content shown from left to right. In general, the higher the carbon or alloy content, the lower the RWAT weight loss. In Figure 3, the data are displayed as a function of R_c macrohardness. Weight loss does not correlate well with R_c since the correlation coefficient r for these data is 0.7, compared to a required value of 0.8 for n = 6 samples (See COO-4246-3 for a discussion of statistical analysis of the wear results).

Table I.

Chemical Analysis of Co-base PM Alloys

	#6	#6HC	#19	#98M2	#3	#Star J
B	.49	.49	.22	.66	.49	.27
C	1.49	1.94	1.88	2.12	2.52	2.67
Co	Bal	Bal	Bal	Bal	Bal	Bal
Cr	28.99	28.99	30.17	30.57	30.91	31.57
Fe	1.46	1.46	1.92	3.09	2.29	.32
Mo	.32	.32	--	.24	.35	.02
Mn	.13	.13	0.65	.23	<.1	.58
Ni	2.13	2.13	1.42	4.04	2.20	1.34
Si	.92	.92	--	.51	.51	.34
V	--	--	--	3.82	--	<.01
W	4.96	4.96	10.37	17.15	11.78	16.94

Table II

Features of the Co-base Powder Metallurgy Alloys

	Type		Microstructure
1.	#6	Low carbide vol. fract.	Low solid solution strengthener content.
2.	#6HC	High carbide vol. fract.	Low solid solution strengthener content.
3.	#19	High carbide vol. fract.	Moderate solid solution strengthener content.
4.	#98M2	High carbide vol. fract.	High solid solution strengthener content.
5.	#3	Very high carbide vol. fract.	High solid solution strengthener content.
6.	#Star-J	Very high carbide vol. fract.	Very high solid solution strengthener content.

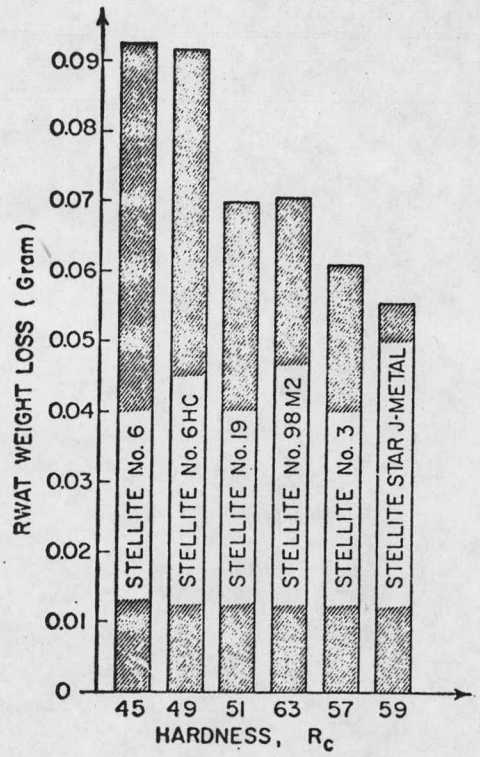

Figure 1. RWAT weight loss of Co-base PM alloys. Carbide volume fraction and/or matrix solid-solution strengthener content increases left to right.

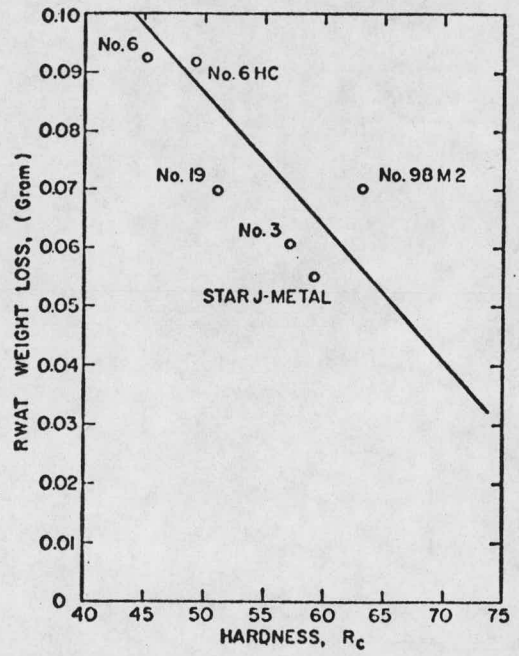

Figure 2. RWAT weight loss of Co-base PM alloys as a function of Rockwell C hardness.

2.3.3 Gouging Abrasion Testing

The GAWT Abrasion Factor for the six Co-base PM alloys is shown in histogram form in Figure 3 and as a function of R_c macrohardness in Figure 4. Both the RWAT (Figure 1) and the GAWT (Figure 3) histograms are constructed with carbide content, matrix alloy content and alloy cost increasing from left to right. The RWAT data lead to the general conclusion that low-stress abrasion resistance improves as alloy cost increases. It is evident that this trend is not as clear for gouging abrasion resistance. The poorer correlation between wear resistance and alloy content in the case of gouging wear is borne out by the plot of abrasion factor vs R_c (Figure 4). The correlation coefficient r for this plot is 0.65, as contrasted with 0.7 for the RWAT plot and desired value of 0.8 for significant correlation as defined in COO 4246-3.

2.3.4 Summary of Wear Testing on PM Alloys.

Both the RWAT and GAWT results lead to the conclusion that macrohardness is a rough predictor of wear resistance, although predictions based on hardness may, especially for the GAWT, be in error by a factor of two. For low-stress abrasion resistance, increasing carbon and alloy content leads to a general improvement in wear resistance. Alloying is not as an effective technique for improving gouging wear resistance.

2.4 Task IV - Wear Scar and Microstructure Characterization

2.4.1 Optical Metallography of Co-base PM Alloys

The six PM alloys were prepared for metallographic examination by standard procedures which included:

1. Coarse wet grinding on 80 to 240 grit SiC belts.
2. Fine wet grinding on 320 to 600 grit SiC papers.
3. Coarse polishing on a nylon cloth* with 6 μm diamond paste abrasive.

*LECLOTH- LECO Corporation, St. Joseph, MI, 49085.

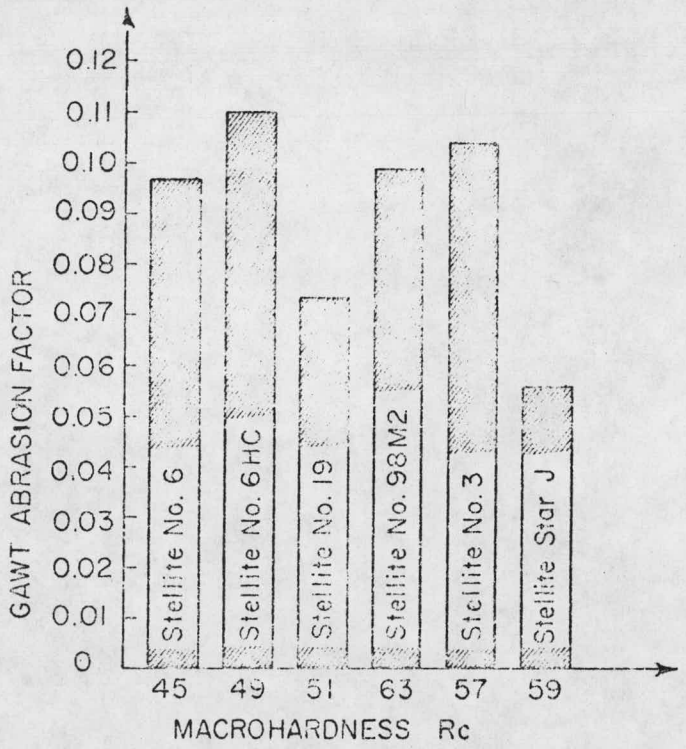

Figure 3. GAWT weight loss of Co-base PM alloys. Carbide volume fraction and/or matrix solid-solution strengthener content increase left to right.

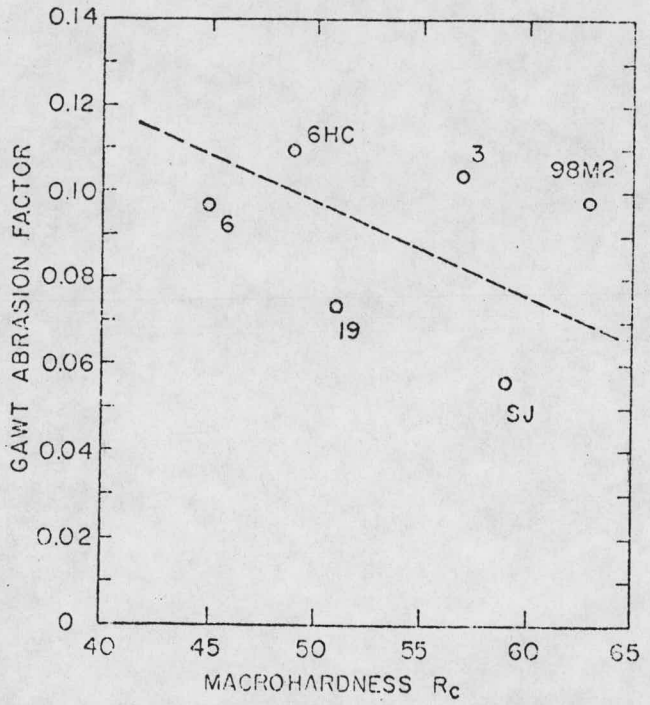

Figure 4. GAWT abrasion factor of Co-base PM alloys as a function of Rockwell C hardness.

4. Fine polishing on LECLOTH* with 0.05 μm γ-Al_2O_3.

5. General etching in 2 volume percent chromic acid in distilled water to reveal grain boundaries.

6. Staining for 5 s in saturated $KMnO_4$ (4 g NaOH, 10 g $KMnO_4$, 85 cm^3 H_2O), to produce contrast between the matrix, Cr_7C_3-type carbides and M_6C-type carbides.

The microstructures of the alloys at 320X and 630X magnification are shown in Figures 5 through 10. The order of increasing carbon and/or alloy content employed in the histograms has been maintained in the figures. In general, the microstructures consist of a FCC Co-rich matrix containing a uniform dispersion of carbides. The only carbide present in alloys 6, 6HC and 19 is of the Cr_7C_3 type, which is elongated in shape and has a roughly hexagonal cross section. In alloys 98M2, 3 and Star J, which contain an excess of 10 weight percent tungsten, dark-staining, roughly cubic $(W,Co)_6C$-type carbides appear.

2.4.2 Quantitative Metallography (QTM) of the Co-base PM Alloys

The microstructures of the PM alloys were analysed quantitatively on a Bausch and Lomb Omicon Alpha image analyser according to techniques described in Report COO-4246-3. The analysis consisted of 100 point measurements on each metallographic sample of the QTM parameters described in the report. Of particular interest were v_f, the carbide volume fraction, and L_a, the projected carbide length per unit area. The volume fraction is of interest since this is a key parameter in theories of dispersion strengthening. The projected length is of interest because it is inversely proportional to carbide size and directly proportional to the carbide/matrix interfacial area. This latter quantity may be significant if the wear mechanisms involve flow-fracture processes (i.e. matrix plowing, carbide spalling) which are easily initiated at the matrix-carbide interface. In addition to v_f and L_a, the porosity remaining after pressing and sintering was obtained.

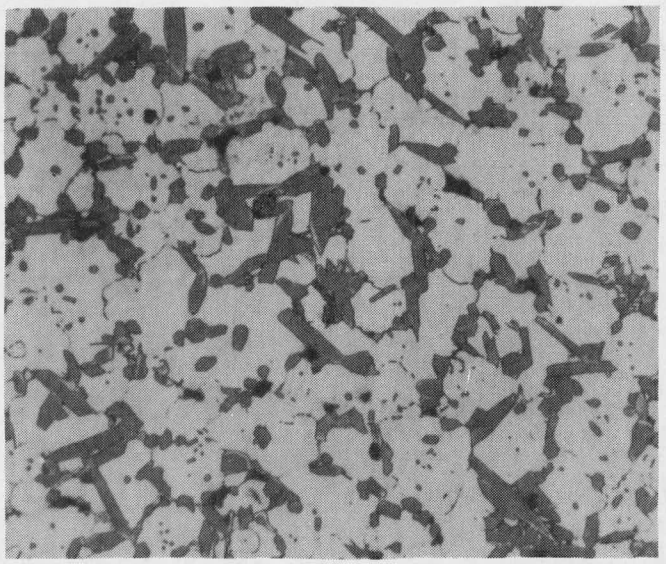

320X

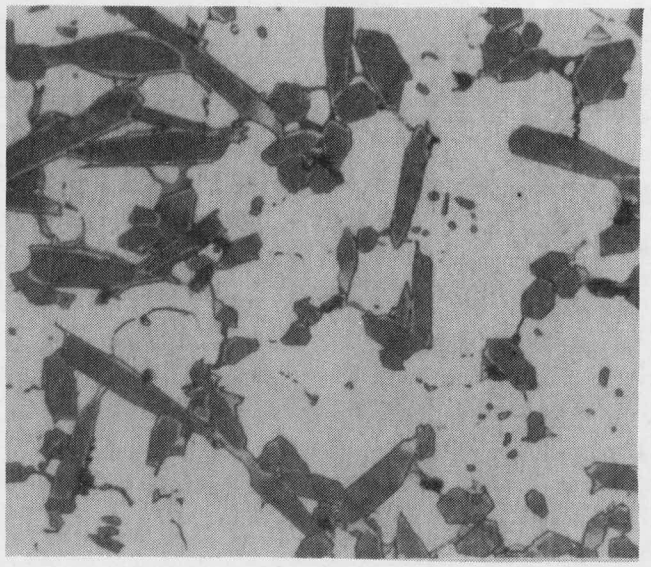

630X

Fig. 5 Microstructure of Stellite No. 6

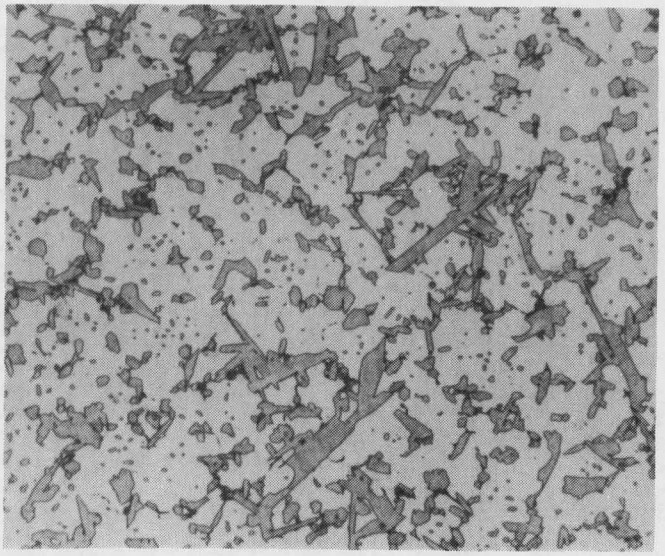

320X

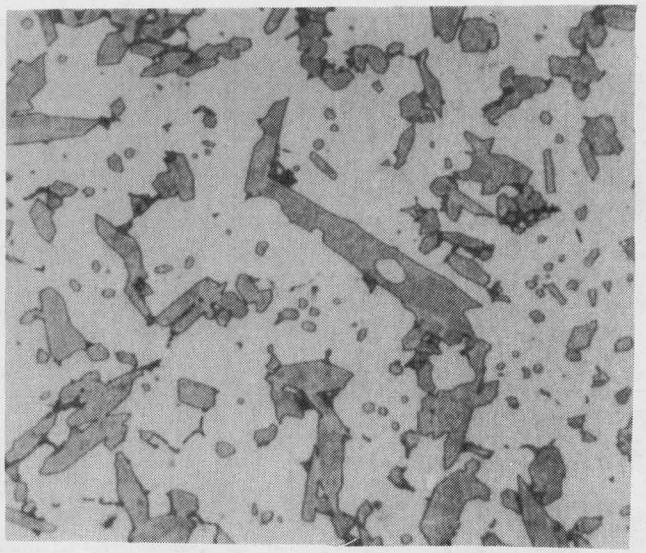

630X

Fig. 6 Microstructure of Stellite No. 6HC

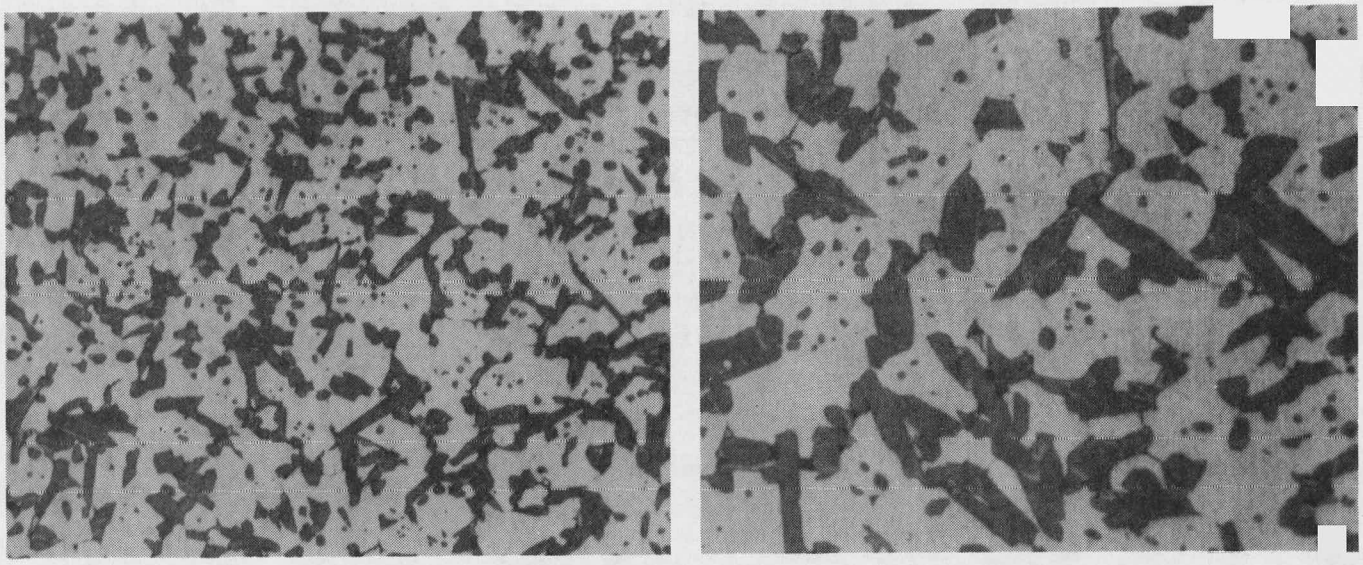

320X 630X

Fig. 7 Microstructure of Stellite No. 19

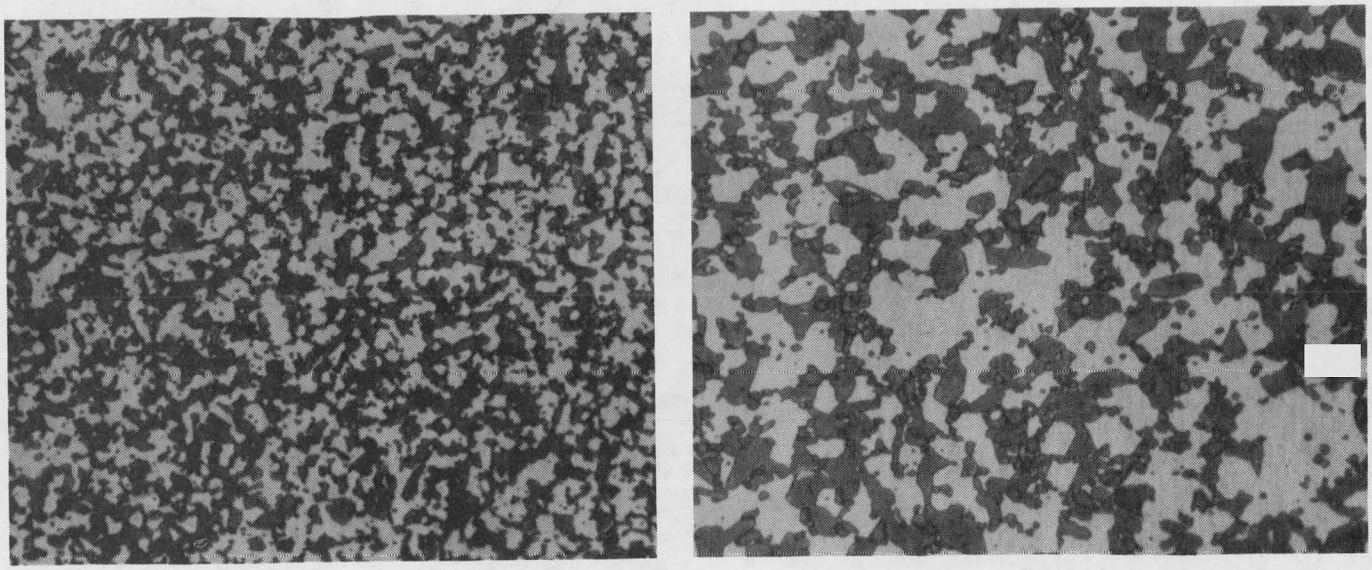

320X 630X

Fig. 8 Microstructure of Stellite No. 98M2

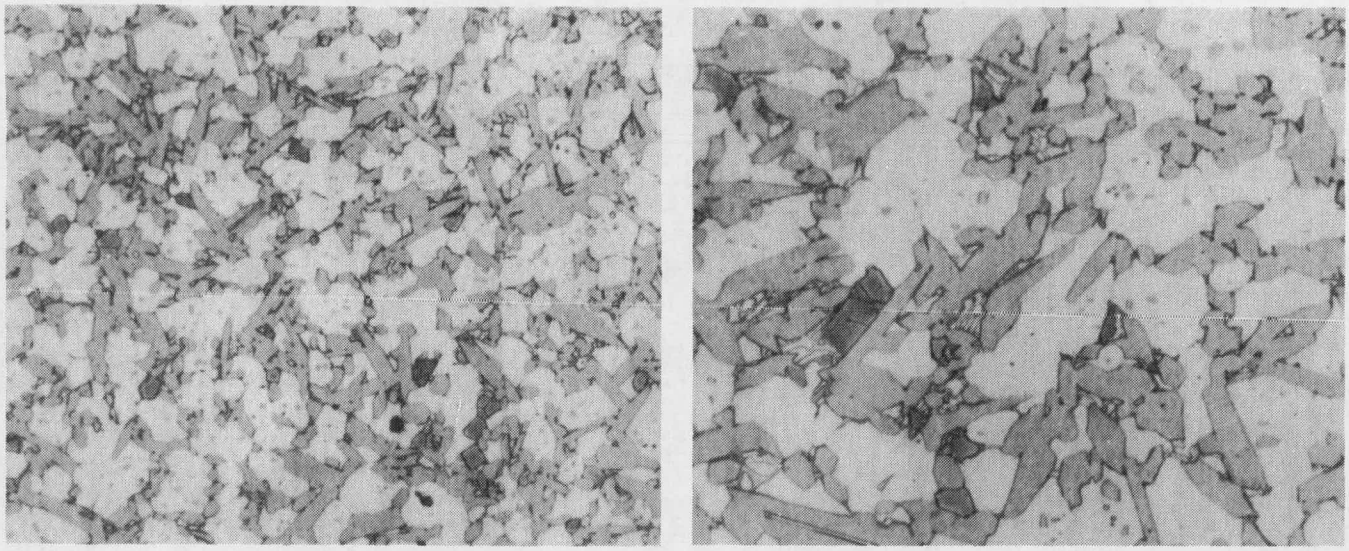

630X

Fig. 9 Microstructure of Stellite No. 3

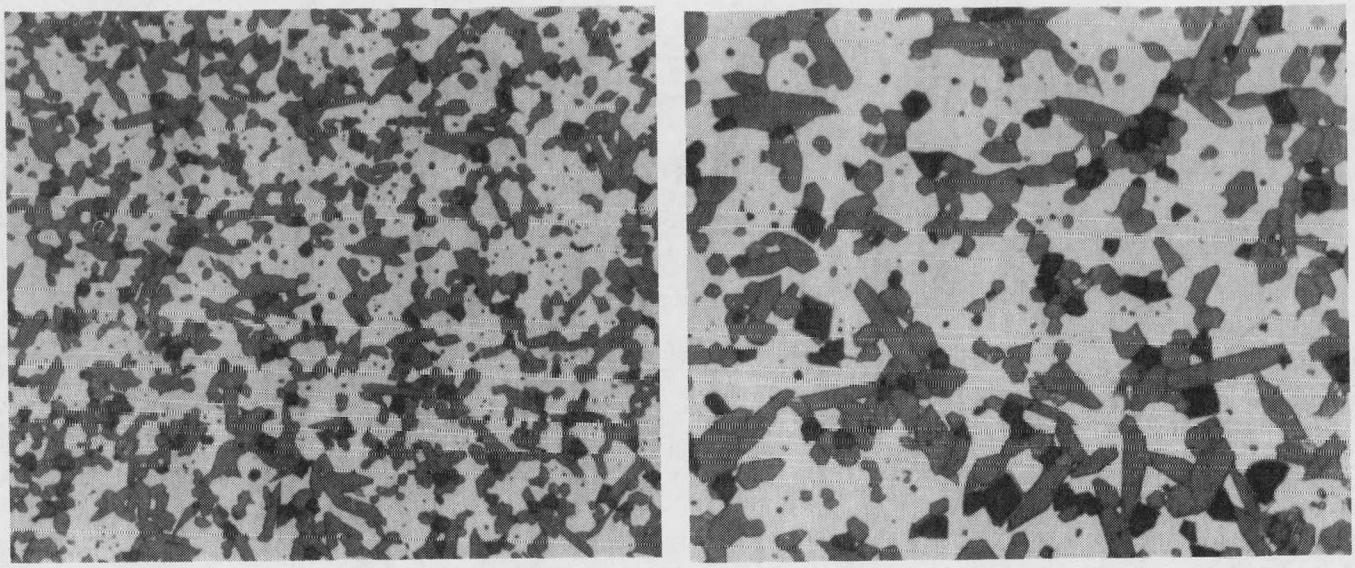

320X 630X

Fig. 10 Microstructure of Stellite Star J-Metal

The QTM results are shown in Table III. As might be expected from the chemical analysis reported in Table I, alloys 98M2, 3 and Star J with higher carbon and tungsten contents show largest v_f. These alloys show a significant fraction of M_6C carbide in addition to Cr_7C_3. The porosity of the less-alloyed materials is about 1 to 2 percent, whereas no porosity is detectable in the highly alloyed materials. The QTM measurements also bear out that which is evident from visual inspection of Figures 5 through 10. Carbide v_f is highest and carbide size ($\sim L_a^{-1}$) is smallest for alloy 98M2.

In a separate study conducted at Stellite Division, Cabot Corporation, Kokomo, IN, electrolytic extraction was employed to collect the carbide phase particles in typical heats of alloys 6, 19 and 3. The carbide lattice parameters, compositions and weight fraction were determined from the extracted powders. These results are presented here in Table IV for the purpose of more completely characterizing the materials under study. The significance of this type of data is yet to be determined.

2.4.3 Wear Scar Microtopography of Co-base PM Alloys

Wear scar micro-profilimetry has been conducted at the Inland Steel Research Laboratories, East Chicago, IN according to the procedure briefly outlined in Report COO-4246-4. The topographic measurements were performed on a Sloan profilometer (with a 0.0127 mm diameter diamond stylus) which is interfaced with a computer for statistical analysis. Surface traces were made across the top of the RWAT wear scars, which is the area where the sand first contacts the specimen. Although a majority of the wear occurs below the entrance region, traces were made at the top because the measurements were not only easier but also more reproducible in the 'flat' region of the test scar. Scans were made at a rate of 1 cm/minute for a total of 2000 points, the computer recording every fourth point.

Table III

Quantitative Metallographic Results for Co-base PM Alloys

Stellite*	Volume Fraction, Percent					Projected Carbide	
	Porosity	Cr_7C_3	M_6C	Total Carbides	σ_v Std. Dev. (%)	Length per Unit Area (cm^{-1})	σ_L Std. Dev. (cm^{-1})
No. 6	1.8	33.8	0	33.8	2.1	0.010	.0007
No. 6HC	1.6	39.5	0	39.5	3.5	0.013	.0013
No. 19	1	37.4	0	37.4	1.4	0.012	.0006
No. 98M2	0	43.6	13	56.6	2.1	0.019	.0004
No. 3	0	46.3	8.9	55.2	5.3	0.011	.0004
Star J-Metal	0	41.0	8.9	49.9	1.3	0.014	.0002

*Stellite Division, Kokomo, IN.

Table IV

Carbides in Typical Sand-cast Co-base Alloys*

	Alloy #6	Alloy #19	Alloy #3
		Lattice Parameter (Å)	
M_7C_3	a_o = 13.999	a_o = 13.981	a_o = 13.995
	C_o = 4.501	C_o = 4.511	C_o = 4.498
M_6C	--	--	a_o = 10.82
	Total Weight Fraction Carbide (M_7C_3 + M_6C)		
	.126	.187	.288
	Total Volume Fraction Carbide (M_7C_3 + M_6C)**		
	.338	.374	.552
	Total Carbide Composition (weight %)		
C	8.12	7.90	7.57
Co	13.88	11.88	13.20
Cr	71.46	68.97	66.76
Fe	0.37	0.45	0.58
Mo	1.14	1.01	0.66
Si	0.29	0.03	0.09
W	4.08	5.58	10.58

*Data obtained at Stellite Division, Cabot Corporation, Kokomo, IN.

**From this project, Table III.

Initially a profile P(I) is drawn and recorded at every point I across the surface. P(I) is then divided into groups of 25-I points and averaged to determine centerline values, C(I). Finally the centerline values, a measure of macrotopography, are subtracted from the profile points P(I) leaving residual microtopography values, R(I). R(I) represents the microtopography of the surface and is the basis for statistical analysis of surface roughness. The critical profile characteristics are:

1) P(I) - actual profile point at I,

2) C(I) = centerline at I (based on 25-point averages), and

3) R(I) = P(I) - C(I) = residual microtopography.

The computer is programmed to calculate three measures of microtopography from these plots: the first is the average absolute displacement from the centerline, AA, which is given by,

$$AA = \left[\sum_{I=1}^{2000} |R(I)| \right] /2000. \qquad (1)$$

The second is the RMS roughness,

$$RMS = \left[\frac{\sum_{I=1}^{2000} (R(I))^2}{2000} \right]^{1/2}. \qquad (2)$$

The third is PPI, the number of peaks per inch scanned.

These three parameters as calculated from the RWAT wear scar traverses on the six PM alloys are listed in Table V, and are plotted against RWAT weight

Table V

Computer-Calculated Microtopography Results on Co -base PM Alloys

Alloy	AA	RMS	PPI	RWAT Weight Loss (g)
6	20.20	38.00	105.60	0.0925
6HC	19.69	26.98	73.60	0.0918
19	21.65	28.06	73.60	0.0634
98M2	11.75	15.41	22.40	0.0701
3	15.91	20.14	35.20	0.0608
Star J	10.30	12.71	12.90	0.0553

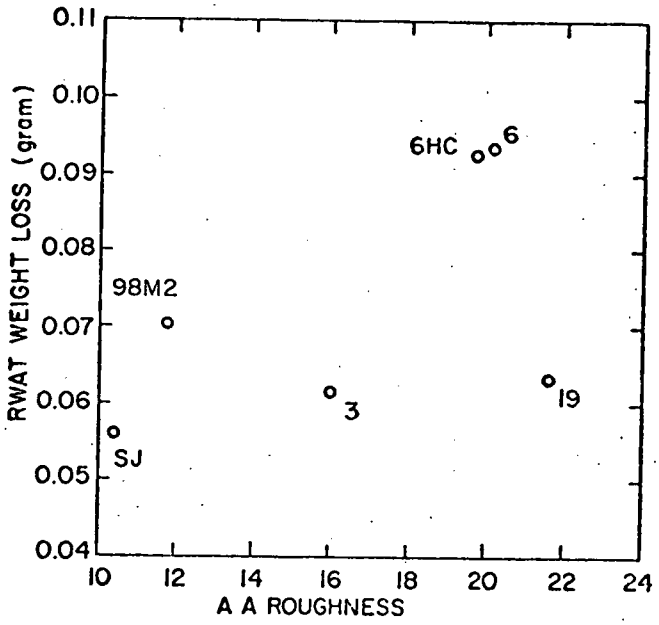

Figure 11. RWAT weight loss vs AA microtopography.

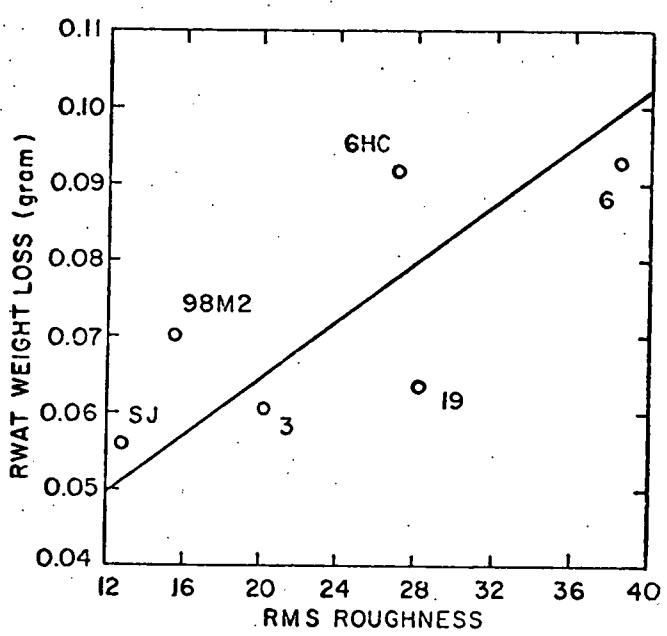

Figure 12. RWAT weight loss vs RMS microtopography.

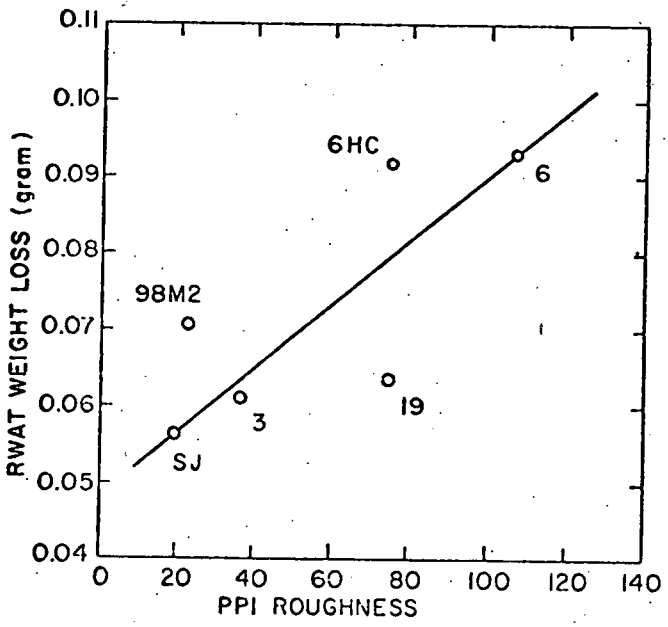

Figure 13. RWAT weight loss vs PPI microtopography.

loss in Figures 11, 12, and 13. RWAT weight loss fails to correlate with AA, shows a rough correlation (r = 0.62) with PPI and a slightly better correlation (r = 0.71) with RMS.

In very general terms, the hardness, microtopography and low-stress abrasion data lead to the conclusion that the harder an alloy, the greater its RWAT wear resistance and the smoother its RWAT wear scar. Attempts to correlate QTM, microtopography, micro- and macrohardness and low-stress abrasion resistance are underway.

2.5 Task V - Analysis of Data

Essentially all effort this quarter has been devoted to data acquisition for the six Co-base PM alloys. Clear structure-property trends emerge from the data, but these remain to be analysed. The general trends are:

1. RWAT weight loss decreases as hardness, carbon and alloy content increase.
2. GAWT weight loss decreases, in a very general sense, as hardness, carbon and alloy content increase.
3. Alloying appears to be an expensive and inefficient means of increasing gouging wear resistance.
4. In low-stress abrasion, abrasion-resistant alloys are characterized by smoother wear scars.

Whether these trends may be quantified in terms of microstructural parameters or flow-fracture theories is to be determined. For example weight loss may be a function of L_a, suggesting that second-phase particle size or degradation process at carbide-matrix interfaces may govern wear. Moreover, wear resistance may be related to the carbide by volume fraction in a power law which follows from dispersion-strengthening theories.

The potential benefit of this type of analysis from both the basic understanding and the alloy design viewpoint is evident from Figure 14, a plot of RWAT weight loss and GAWT abrasion factor as a function of v_f. A minimum in wear (or maximum in wear resistance) appears at about 50% v_f for both types of wear. From the design viewpoint, alloying beyond this v_f to increase matrix strength and/or carbide volume fraction is counterproductive if maximum low-stress or gouging wear resistance is desired. Furthermore, low-stress and gouging wear are usually considered two fundamentally different phenomena, yet these data suggest that they may be governed by common flow-fracture processes.

3. SUMMARY

Research in this quarter has been concentrated on Co-base PM alloys. It has been found that low-stress abrasion resistance correlates roughly to alloy macrohardness, but gouging wear resistance may only be predicted from hardness data to within a factor of two. It appears that alloying to improve gouging wear resistance is expensive and inefficient. Capability for optical and quantitative metallography analysis of the alloys has been established and key QTM parameters have been measured.

Of particular interest in the data generated in this quarter is the apparent correlation of wear scar microtopography to wear resistance. In addition, the finding that maximum wear resistance is obtained at some intermediate carbide volume fraction provides quantitative information for alloy design and suggests that similar flow-fracture processes may govern low-stress and gouging abrasive wear.

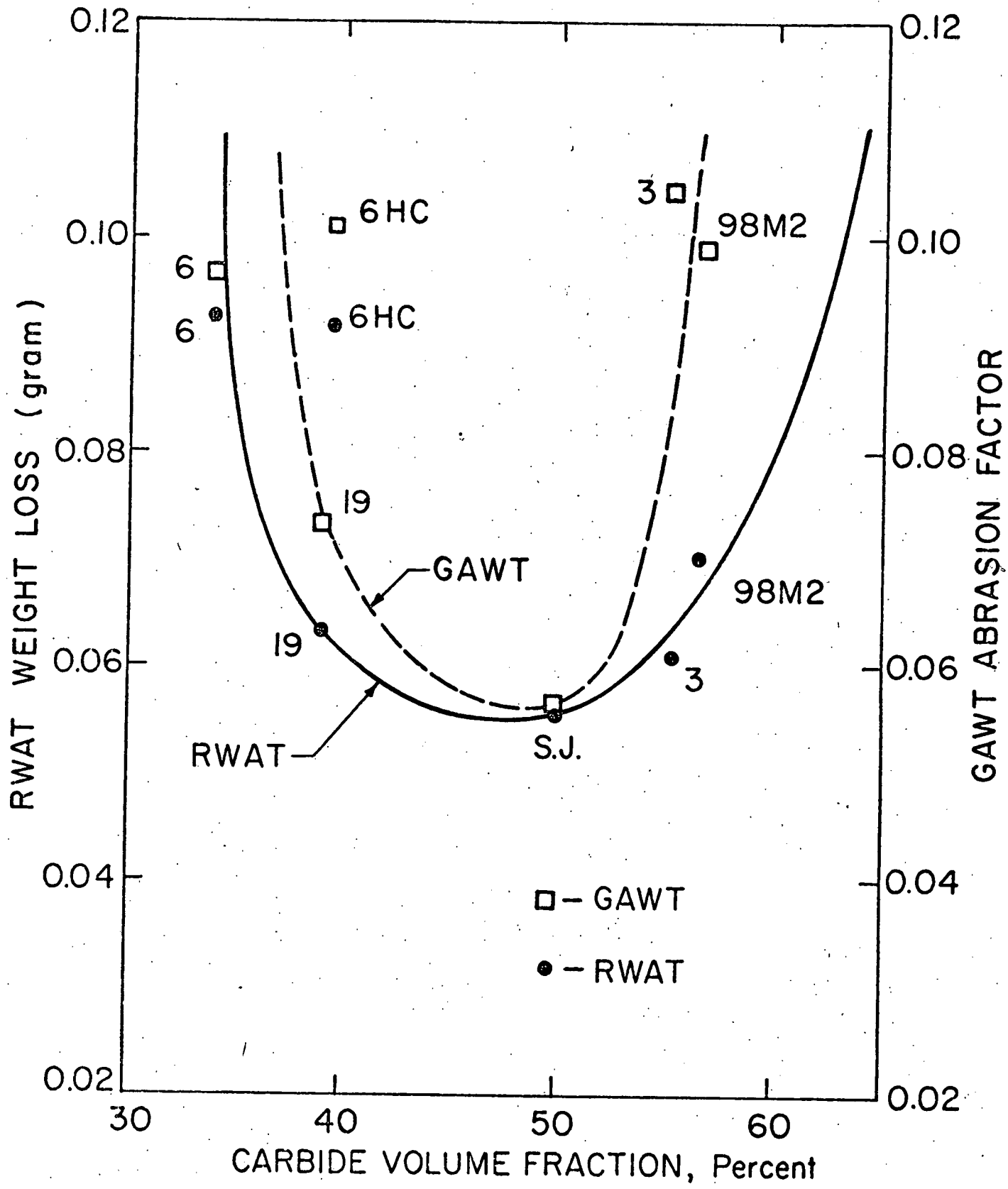

Figure 14. RWAT weight loss and GAWT abrasion factor as a function of carbide volume fraction for the Co-base PM alloys.

4. PERSONNEL

The principal investigator, Dr. N. F. Fiore, has spent about one-fifth effort on the project during this quarter of the academic year. Mr. Stephen Udvardy (M.S. candidate) has devoted half-time effort to the project, and Mr. Joseph Coyle, Project Engineer, has devoted full-time to the project.

LIST OF TABLES

LIST OF FIGURES

Form ERDA-427
(2/76)
ERDAM 3201

U. S. ENERGY RESEARCH & DEVELOPMENT ADMINISTRATION

UNIVERSITY–TYPE CONTRACTOR'S RECOMMENDATION FOR DISPOSITION OF SCIENTIFIC AND TECHNICAL DOCUMENT

(See Instructions on Reverse Side)

1. ERDA REPORT NO.
COO-4246-5

2. TITLE
Microstructural Effects in Abrasive Wear

3. TYPE OF DOCUMENT (Check one):

☒ a. Scientific and technical report
☐ b. Conference paper:

Title of conference _____

Date of conference _____

Exact location of conference _____

Sponsoring organization _____

☐ c. Other (Specify)

4. RECOMMENDED ANNOUNCEMENT AND DISTRIBUTION (Check one):

☒ a. ERDA's normal announcement and distribution procedures may be followed.
☐ b. Make available only within ERDA and to ERDA contractors and other U. S. Government agencies and their contractors.

5. REASON FOR RECOMMENDED RESTRICTIONS:

N/A

6. SUBMITTED BY: NAME AND POSITION (Please print or type)

Nicholas F. Fiore
Professor and Chairman

Organization

Department of Metallurgical Engineering & Materials Science
University of Notre Dame
Notre Dame, Indiana 46556

Signature N.F. Fiore

Date 7/1/78

FOR ERDA USE ONLY

7. ERDA CONTRACT ADMINISTRATOR'S COMMENTS, IF ANY, ON ABOVE ANNOUNCEMENT AND DISTRIBUTION RECOMMENDATION:

8. PATENT CLEARANCE:

☐ a. ERDA patent clearance has been granted by responsible ERDA patent group.
☐ b. Report has been sent to responsible ERDA patent group for clearance.
☐ c. Patent clearance not required.

DISTRIBUTION LIST

Mr. John J. Mahoney
Senior Contract Administrator
Contracts Management Office
DOE - Chicago Operations Office
9700 South Cass Avenue
Argonne, IL 60439
- 6 copies -

Dr. Thomas Cox
DOE - Fossil Energy Research
Room 4203
20 Massachusetts Avenue
Washington, D.C. 20545
- 3 copies -

Dr. Paul Scott
DOE - Fossil Energy Research
20 Massachusetts Avenue
Washington, D.C. 20545

Dr. Sam Schnedier
National Bureau of Standards
Washington, D.C. 20234

Dr. John Dodd
Climax Molybdenum Company
13949 West Colfax Avenue
Golden, CO 80401

Metals and Ceramics Information Center
Battelle-Columbus Laboratories
505 King Avenue
Columbus, OH 43201

Dr. J. L. Parks
Climax Molybdenum Research Lab.
1600 Huron Parkway
Ann Arbor, MI 48106

Dr. M. S. Bhat
Materials and Molecular Research
Bldg. 62 - Room 239
Lawrence Berkeley Laboratory
University of California
Berkeley, CA 94720

Mr. Howard Avery
69 Alcott
Mahwah, N.J. 07430

Dr. Kenneth Anthony
Stellite Division
Cabot Corporation
Kokomo, IN 46901

Dr. Stanley Wolf
Materials Science Program
Division of Basic Energy Sciences
DOE
Washington, D.C. 20545

Dr. Joseph Klein
Stellite Division
Cabot Corporation
Kokomo, IN 46901

Dr. Jerry L. Arnold
Research and Technology
Armco Steel Corporation
Middletown, OH 45043